Int J Clin Exp Med 2017;10(9):13213-13223
www.ijcem.com /ISSN:1940-5901/IJCEM0052960

Original Article

The protective role of remote ischemic preconditioning in a rat model of gastric ischemia-reperfusion injury by inhibiting nuclear factor κB expression

Dao-Ri-Na Bao[1], Yu-Qin Jia[2], Yan-Mei Liu[2], Heng-Bin Li[2], Peng-Fei Wu[2], Jing Pan[2], Xiao-Xue Wang[2], Si-Yu Wei[2], Xing-Yong Wang[3]

[1]Chongqing Medical University, Chongqing 400016, P. R. China; [2]Intensive Care Unit, The Second Affiliated Hospital of Inner Mongolia Medical University, Hohhot 010031, P. R. China; [3]Emergency Department, Children's Hospital of Chongqing Medical University, Chongqing 400014, P. R. China

Received June 22, 2016; Accepted July 23, 2017; Epub September 15, 2017; Published September 30, 2017

Abstract: Objective: This study aims to discuss the role of remote ischemic preconditioning (RIPC) in gastric ischemia-reperfusion injury (GI-RI) through regulating nuclear factor kappaB (NF-κB). Method: A total of 114 healthy male SD rats were randomly divided into sham group (n = 6), I/R group (n = 36), RIPC group (n = 36) and NF-κB activation + RIPC group (n = 36). I/R, RIPC group, NF-κB activation + RIPC group were assigned into 6 sub-groups including reperfusion for 0 hour (T0), 1 hour (T1), 3 hours (T3), 6 hours (T6), 12 hours (T12) and 24 hours (T24). After 6 hours of reperfusion, the histopathological changes in gastric mucosal tissues were recorded and cell apoptosis was detected. At different time points after reperfusion, the gastric mucosal damage index (GMDI), malondialdehyde (MDA) level and superoxide dismutase (SOD) activity was determined. NF-κB p65 protein expression was detected using immunohistochemistry and Western blotting analysis. Results: The RIPC group showed slighter gastric mucosal damage than the I/R group. There were significantly higher GMDIs and MDA levels, decreased SOD activity and a higher NF-κB p65 protein expression in the I/R and NF-κB activation + RIPC groups compared to the sham group. The RIPC group displayed decreased cell apoptosis and MDA levels and increased SOD activity and NF-κB p65 protein expression in comparison to the I/R and NF-κB activation + RIPC groups. At T0, T1, T3 and T6, the RIPC group showed significantly lower GMDIs than the I/R and NF-κB activation + RIPC groups. Conclusion: RIPC may protect against GI-RI by inhibiting NF-κB activation and decreasing oxygen free radicals and neutrophil infiltration.

Keywords: Remote ischemic preconditioning, gastric, ischemia-reperfusion injury, nuclear factor κB, malondialdehyde, superoxide dismutase, apoptosis, neutrophil granulocyte

Introduction

Ischemia-reperfusion injury (IRI) results from a prolonged ischemic insult followed by a restoration of blood perfusion. This can affect all oxygen dependent cells relying on an uninterrupted blood supply and thereby damage aerobically metabolizing organs and tissues [1]. Gastric ischemia-reperfusion injury (GI-RI) can be induced by many stress conditions such as hemorrhagic shock, major surgery, sepsis, burns, ischemia and trauma [2]. In relative oxygen species, microvascular dysfunction, polymorphonuclear leukocyte infiltration and decreased prostaglandin concentrations may play a role in the pathogenesis of gastric mucosal injury through ischemia-reperfusion [3-6]. Current research concerning GI-RI mentions its pathogenic and underlying molecular mechanisms [3, 7, 8]. Remote ischemic preconditioning (RIPC) is a systemic strategy for organ protection whereby brief limb ischemia brings systemic protection against prolonged ischemia in distant organs [9]. The effects of RIPC occur through the recruitment of either the neuronal pathway or humoral mediators. The most evident beneficial effects are observed on the myocardium [10]. RIPC has been widely applied to protect organs and tissues from acute injury during surgeries such as the myocardium, kidney and coronary artery [11-13]. This has aroused wide concern in the field of organ protection. Pickard et al. revealed that RIPC can protect the brain and liver from I-RI [14, 15]. Bobryshev et al. also

reported a protective role of RIPC in gastric mucosa [16]. However, the protective value of RIPC in GI-RI still remains unclear.

Nuclear factor kappaB (NF-κB) is a family of dimeric transcription factors found in all cells and interacts with the immunoglobulin light-chain enhancer of B cells [17]. And here 5 distinct NF-κB proteins, namely NF-κB1 (p50 and p105), NF-κB2 (p52 and p100), RelA (p65), c-Rel and RelB constitute the NF-κB transcription factor family among mammals [18]. The NF-κB pathway is considered a prototypical pro-inflammatory signaling pathway which plays a critical role in the expression of pro-inflammatory genes such as chemokines, cytokines and adhesion molecules [19]. Interestingly, NF-κB enhances the apoptosis and damage of gastric mucosal cells [20]. GI-RI is related to changes in gastric mucosal cellular proliferation and apoptosis induced by ischemia-reperfusion. To better understand the causes of GI-RI it is necessary to study the specific molecule involved in proliferation and apoptosis [2]. Furthermore, the effect of RIPC on NF-κB activation has been proposed to attenuate lipopolysaccharide-induced liver injury [21]. However, no study has demonstrated the association between RIPC, NF-κB activation and GI-RI. Therefore, in the present study we aim to investigate the effect of RIPC on gastric mucosal tissue NF-κB p65 expression and the potential role of RIPC in rats with GI-RI.

Materials and methods

Ethics statement

This experiment was performed with the approval of the Ethics Committee (approval number: 2015016) and animal experiments were conducted in conformity with the Helsinki Declaration.

Experimental animal and grouping

A total of 114 healthy male Sprague-Dawley (SD) rats aged 9 to 11 weeks weighing 230 ± 20 g were used in the experiment. They were fed every 12 hrs at room temperature with a relative humidity of 20% to 50%. Before the experiment, the rats were fasted for 24 hrs but drank water freely. All rats were obtained from the Experimental Animal Center of Children's Hospital of Chongqing Medical University. All rats were randomly divided into 4 groups: the sham operation (sham) group (n = 6), the ischemia/reperfusion (I/R) group (n = 36), the remote ischemic preconditioning (RIPC) group (n = 36) and the nuclear factor Kappa B (NF-κB) activation + RIPC group (n = 36). Rats were randomly selected from the I/R, RIPC and the NF-κB activation + RIPC groups and the injury induced by gastric ischemic-reperfusion was observed at different time points after I/R. Firstly, 0.5 hrs of ischemia was performed on the rats. Subsequently, records were taken after 0 hr of reperfusion (T0), 1 hr of reperfusion (T2), 3 hrs of reperfusion (T3), 6 hrs of reperfusion (T6), 12 hrs of reperfusion (T12) and 24 hrs of reperfusion (T24).

Gastric ischemic-reperfusion injury (GI-RI) rat models

To construct GI-RI rat models, 6 rats in the I/R group were injected intraperitoneally with 10% chloral hydrate (300-350 mg) (Sigma-Aldrich Co., St Louis MO, USA) for general anesthesia [22]. The rats were placed on a heating blanket (37°C) to maintain their body temperature and then fixed on the operating table in a supine position. With a median incision through the linea alba, the celiac arteries were separated from the abdominal aorta and clamped using a small bulldog clamp for 30 mins. After removing the clamp, the celiac arteries were reperfused for 0 hr, 1 hr, 3 hrs, 6 hrs, 12 hrs and 24 hrs. The celiac arteries of 6 rats in the sham group were separated without clamping. In the RIPC group, the hepatic artery and portal vein of 6 rats were clamped for 5 mins and then reperfused for 10 mins. This was performed twice [23], and the following steps were the same as the I/R group. In the NF-κB activation + RIPC group, the NF-κB activation was induced with Helicobacter pylori (HP), with the following steps the same as the RIPC group. HP containing vancomycin (10 mg/L), amphotericin B (10 mg/L), polymyxin B (2500 U/L) and trimethoprim (5 mg/L) and 7% nonfiber goat blood were put in a Columbia blood agar plate, and then incubated in the micro aerobic environment (10% CO_2, 5% O_2, 85% N_2) at 37°C. After 48 hrs of culture, normal saline free of bacterium was used for HP washing. The broth concentration was adjusted as 1×10^9 CFU/mL, and the intragastric administration was conducted at the interval of 48 hrs with 5 times in

total. The success criteria for GI-RI model construction were as follows: the serum color of rat's stomach gradually changed from scarlet to dark purple when the celiac arteries were clamped, the color of rat's stomach immediately reverted back to its original color (dark purple to scarlet) when the clamp was removed and reperfusion was performed 1 to 3 hrs after the operation, and the rat woke up from anesthesia and gradually resumed normal activities. The criteria for unsuccessful GI-RI model establishment was: 5 mins after reperfusion, no color reversion was seen in rat's stomach, peripheral tissues or organs were injured during the operation or 1 to 3 hrs after operation unless the rat did not wake up from anesthesia or died. At six time points of reperfusion (T0, T1, T3, T6, T12 and T24) the stomach of rats in the sham group, I/R group, RIPC group and NF-κB activation + RIPC group were taken out and the gastric mucosal damage index (GMDI) was recorded to assess the extent of GI-RI. Specimens of gastric mucous were randomly divided into two parts. One part of the specimen was stored in a -80°C freezer after removal and the remainder was sliced, paraffin-embedded and fixed in 10% neutral formalin (Nanjing Jiancheng Bioengineering Institute, Jiangsu, China).

Histopathological observation

A portion of gastric mucous specimens from the four groups (the sham group, the I/R group, the RIPC group and the NF-κB activation + RIPC group) were fixed in 10% neutral formalin for 24 hrs. The tissues were dehydrated in ethanol, cleared, de-waxed, paraffin-embedded, sliced into 4 μm sections and then hematoxylin-eosin (HE) staining was performed. Tissue sections were de-waxed and rehydrated with double-distilled water followed by gradient ethanol dehydration. This involved xylene I for 15 mins, xylene II for 15 mins, absolute alcohol I, absolute alcohol II, 95% alcohol I, 95% alcohol II, 80% alcohol (dehydrated for 2-5 mins in each step) and finally rinsed with double-distilled water. Tissue sections were stained with hematoxylin for 5 mins, rinsed with water, differentiated by 1% hydrochloric acid alcohol and re-rinsed with water. The color of tissue sections reverted to blue with ammonia water. Tissues were also counterstained with eosin for 3 mins and rinsed with water. Afterwards, they were dehydrated with gradient ethanol (80% alcohol, 95% alcohol I, 95% alcohol II, absolute alcohol I and absolute alcohol II for 2-3 mins in each step). Tissue sections were also cleared in xylene twice for 10 mins in total. After removing the xylene around the sections, neutral gum was added into the sections and sealed with a coverslip. The double-blind method was applied to observe the gastric mucous histopathological changes under an optical microscope. Xylene, ethanol, hematoxylin, eosin and neutral gum were bought from Sigma-Aldrich, Inc. (St Louis MO, USA). The LM1235 paraffin section machine was provided by Leica Co., German. The KD-MB paraffin embedding machine utilized was from Jinhua kennono electronics technology Co., Ltd. (Zhejiang, China) and the optical microscope CX-31 was purchased from Olympus Optical Co., Ltd. (Tokyo, Japan).

Western blotting

Gastric mucosal tissue specimens (100 mg) were cut into small pieces and put into a homogenizer for protein extraction. Lysate and phenylmethyl sulfonylfluoride (PMSF) were added, and then the specimens were homogenized at 4°C for 30 mins and then centrifuged (15000 r/min) to obtain the supernatant. The proteins in the nucleus were extracted using a nuclear extract kit (Active Motif, Carlsbad, CA). Cells in each group were washed twice with precooled Tris-buffered saline (TBS), 400 μl of solution A was added, and cells were then suspended and then bathed in ice for 15 mins. After being mixed with 25 μl of 10% NP40 solution, the cells were centrifuged at 5000 r/min at 4°C. After the addition of 30 μl of solution B, the cells were re-suspended and shaken at 4°C for 15 min. Subsequently, the supernatant was obtained through centrifugation (5000 r/min at 4°C for 10 mins) and stored in a liquid nitrogen or a -80°C refrigerator. The protein content was detected using a bicinchoninic acid (BCA) protein concentrations detection kit (Beyotime Biotechnology Institute, Shanghai, China). A 5 × loading buffer (Beyotime Biotechnology Institute, Shanghai, China) was added into the supernatant and then mixtures were boiled for 5 mins to denaturalize the protein. Equivalent quantities of proteins (100 ug proteins per lane) were separated using 10% sodium dodecylsulphate-polyacrylamide gel electrophoresis (SDS-PAGE) and electro-transferred onto a nitrocellulose (NC) membrane (Amresco, USA). The NC membrane with transferred proteins was blocked with 5% skimmed milk at

room temperature, added to the primary antibody (mouse anti-NF-κB antibody; 1: 1000) which was diluted with Tris buffer saline plus tween 20 tris (TBST) (Beijing Elisakit Technology Co., Ltd.) and left overnight at 4°C. The transfer membrane was rinsed with a TBST solution 3 times for 5 mins each time. Subsequently, the secondary antibody (goat anti-mouse IgG-horseradish peroxidase) was added for a 2 hrs reaction at 37°C. The membrane was then re-rinsed with TBST. An even amount ofchromogenic substrate solutions A and B (Promega Corp., Madison, Wisconsin, USA) were mixed together, developed at room temperature for 1 min, sealed with plastic wrapping film and stored in a darkroom. After developing and fixing the exposed X-ray films a band analysis for NF-κB (p65) protein expression was conducted using the Gel-Pro analyzer 4.0 image analysis software. With glyceraldehyde-3-phosphate dehydrogenase (GAPDH) as an internal reference, the protein expression of NF-κB p65 was determined using the gray value ratio of GAPDH/the target protein. The primary and secondary antibodies were purchased from KangChen Bio-tech Inc., Shanghai, China, the springboard decolorization shaker (ZD-9500) was purchased from Hualida Biotechnology Co., Ltd., Taicang, China and the vertical electrophoresis tank was purchased from Bio-Rad Laboratories, Inc., Hercules, CA, USA.

Immunohistochemistry (IHC) assay

The gastric mucosal tissue sections were dewaxed, hydrated and boiled in a citrate buffer solution (pH = 6.0) for 15 mins for antigen retrieval. After this process, the endogenous peroxidase was deactivated. The primary antibody (mouse anti-rat NF-κB antibody from Santa Cruz Biotechnology, Inc., Santa Cruz, CA, USA) and secondary antibody (goat anti-mouse IgG-horseradish peroxidase conjugate from Santa Cruz Biotechnology, Inc., Santa Cruz, CA, USA) was added in order of priority and then diaminobenzidine (DAB) staining and hematoxylin counterstaining were performed. After gradient ethanol dehydration, the gastric mucosal sections were sealed using neutral gum. The primary antibody was replaced with PBS as a negative control. If colloid particles were observed in the cell or brown granules were observed in the nucleus, the cell was regarded as a positive cell. The number positive cells containing NF-κB p65 divided by the total number of cells in the same visual field under high magnification was considered to be the relative expression of NF-κB p65. Three gastric mucosal sections were randomly selected for each group and 10 visual fields were randomly selected for each section. The average positive cell rate was analyzed. PBS, citrate buffer solution and the DAB chromogenic reagent kit were purchased from Beijing Zhongshan Biotechnology Co., Ltd.

Gastric mucosal damage assessment

After anesthesia, the rat abdominal cavities were opened, and their stomachs were removed, cut along the greater curvature and rinsed in cold normal saline. The stomachs were then placed on an ice tray and the lesions were scored with a graticule (1 mm^2 per pane) under a microscope. They were assessed using cumulative length scores based on pin-point erosions, ulcers and hemorrhagic spots within the gastric epithelium. 0 points represented a lesion length ≤ 1 mm, 1 point represented a lesion length of > 1 mm and ≤ 2 mm, 2 points represented a lesion length of > 2 mm and ≤ 3 mm, 3 points and beyond were scored in the same manner. If the width of the lesion exceeded 1 mm the score was doubled. The average cumulative length scores were obtained using the GMDI of each group [22].

TdT-mediated dUTP nick-end labeling (TUNEL) method

The tdT-mediated dUTP Nick-End Labeling (TUNEL) method was applied to detect gastric mucosal cells apoptosis (the TUNEL detection kit was bought from Wuhan Boster Bioengineering Co., Ltd., Hubei, China). The coverslips were rinsed with a 30% Triton X-100 solution for 5 mins, and then washing with phosphate buffer saline (PBS) three times. 100 μl of TUNEL reaction solutions were added to cover the gastric mucosal cells whilst being kept away from light for 1 hr at 37°C. The reaction was terminated using a terminal solution for 15 mins at room temperature and then coverslips were re-rinsed with PBS three times. Subsequently, gastric mucosal cells were stained with 200 μl of 4',6-diamidino-2-phenylindole (DAPI) for 6 mins at room temperature and then rinsed with PBS three times. Under a fluorescence microscope, visual fields were randomly selected, and the number of positive apoptotic cells and

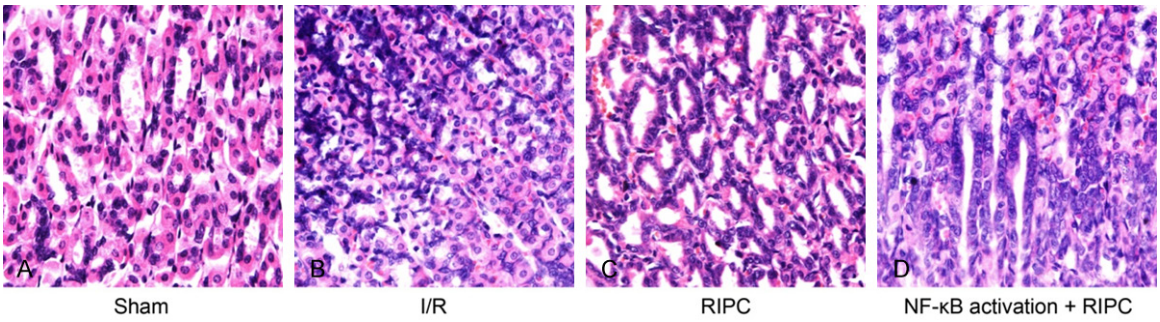

Figure 1. Histopathological changes of gastric mucosa tissue of rats among the sham (A), I/R (B), RIPC (C) and NF-κB activation + RIPC (D) groups at the time point of T6 under a light microscope (HE staining × 200). Notes: I/R, ischemia/reperfusion; RIPC, remote ischemic preconditioning; NF-κB, nuclear factor kappaB.

total cells were counted. The apoptosis rate = positive apoptotic cells/total cells × 100%.

Detection of gastric mucosal superoxide dismutase (SOD) activity and malondialdehyde (MDA) levels

After the rat stomachs were excised, an incision was made along the lesser curvature and rinsed in normal saline. Gastric mucosa sections of the greater curvature were obtained to prepare 1% homogenate with cold normal saline. The homogenate was randomly selected (30 ul for each sample) and the SOD detection kit was used to detect the total SOD and Cu-Zn SOD activities (Nanjing Jiancheng Bioengineering Institute, Jiangsu, China). Gastric mucosa sections were obtained using the same procedure as above and prepared into 10% homogenate with cold normal saline. The homogenate was randomly selected (200 ul for each sample) and the MDA detection kit (Nanjing Jiancheng Bioengineering Institute, Jiangsu, China) was used to detect the MDA level.

Statistical analysis

The SPSS version 20.0 software (SPSS, Inc., Chicago, IL) was used for data analysis. Measurement data were presented as mean ± standard deviation ($\bar{x} \pm s$). The independent samples *t*-test was performed among groups. Enumeration data were expressed as a ratio or percentage and the chi-square test was performed to analyze this data. Repeated-measures data within groups was analyzed to detect the repeated-measures analysis of variance. To analyze the comparison of GMDI, positive cell rate and the NF-κB p65 protein expression between each group, one-way analysis of variance (ANOVA) and the bonferroni's test was utilized. A $P < 0.05$ was considered to be statistically significant.

Results

Histopathological changes of rat gastric mucosa tissue among the sham, I/R, RIPC and NF-κB activation + RIPC groups

All rats had good appetites, mental status and no rat died during or after the operation. There was a 100% success rate in GI-RI model establishment. The histopathological changes in rat gastric mucosa tissues at time point T6 is presented as follows: In the sham group, there was a smooth gastric mucosa, integrated epithelium and orderly distribution of glands. In the I/R group, rats exhibited severe gastric mucosal damage, edema, congestion, erosion, disintegration in the mucosal glands, eosinophils, neutrophils between the muscular layer and glands and congestion in the interstitial blood vessels. In comparison to the I/R group, the RIPC group showed a lower degree of gastric mucosal damage, milder edema and congestion of mucosal glands, fewer eosinophils and neutrophils between muscular layers and glands as well as a milder congestion in the interstitial blood vessels ($P < 0.05$). No significant difference was observed between the I/R and NF-κB activation + RIPC groups concerning the degree of gastric mucosal damage, edema, congestion, erosion and disintegration of mucosal glands, congestion in the interstitial blood vessels and number of eosinophils and neutrophils ($P > 0.05$) (**Figure 1**).

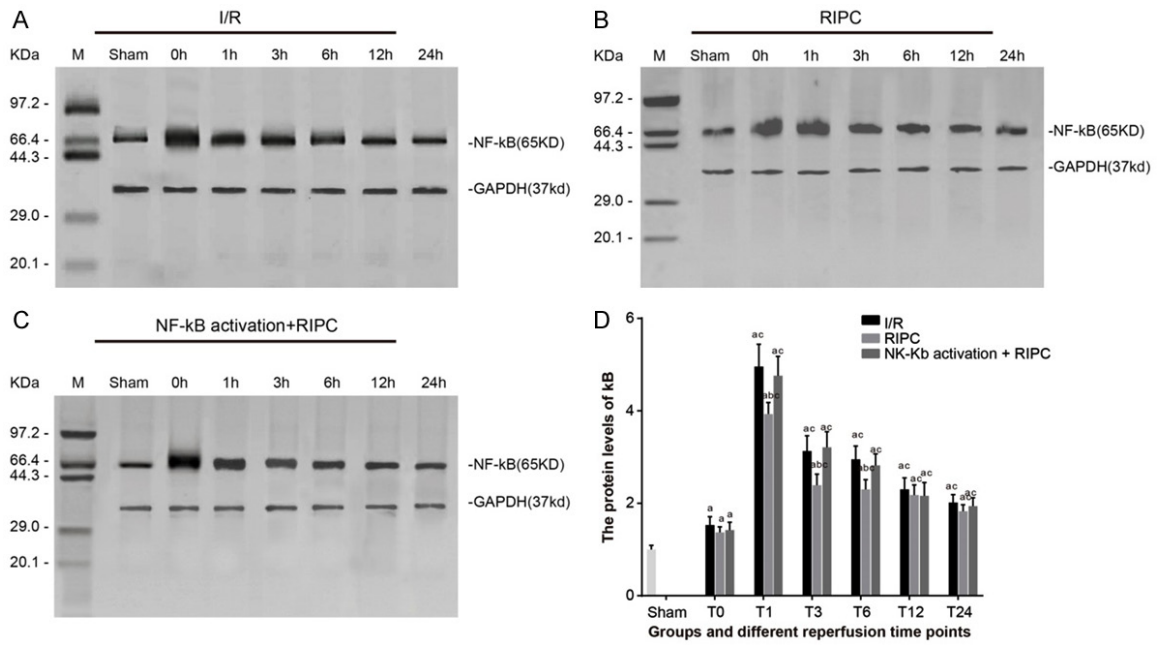

Figure 2. Protein expressions of NF-κB p65 in the nucleus among the sham, I/R, RIPC and NF-κB activation + RIPC groups. Notes: I/R, ischemia/reperfusion; RIPC, remote ischemic preconditioning; NF-κB, nuclear factor kappaB; compared with sham group, $^{a}P < 0.05$; compared with I/R group and NF-κB activation + RIPC group at the same time points, $^{b}P < 0.05$; compared within groups at T0, $^{c}P < 0.05$.

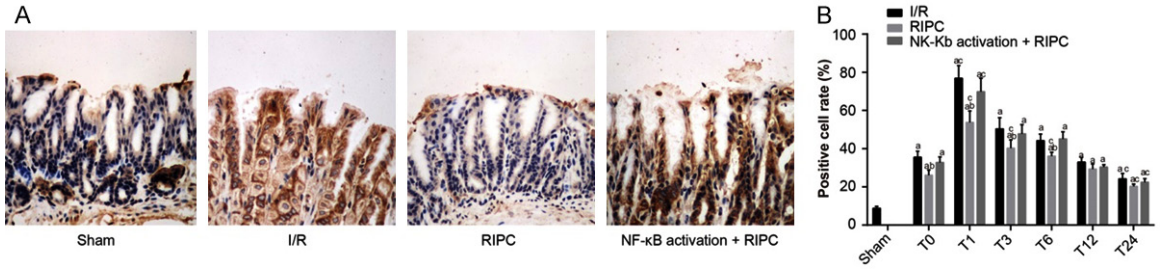

Figure 3. Immunohistochemical staining (A) and the positive cells rate (B) in different groups. Notes: I/R, ischemia/reperfusion; RIPC, remote ischemic preconditioning; NF-κB, nuclear factor kappaB; compared with sham group, $^{a}P < 0.05$; compared with I/R group and NF-κB activation + RIPC group at the same time points, $^{b}P < 0.05$; compared within groups at T0, $^{c}P < 0.05$.

Protein expressions of NF-κB p65 in the nucleus among the sham, I/R, RIPC and NF-κB activation + RIPC groups

The optical density (OD) value showed that, among the six time points (T0, T1, T3, T6, T12 and T24), the NF-κB p65 protein expression in the nucleus was highest at T1 and lowest at T24 in the I/R, RIPC and NF-κB activation + RIPC groups. The protein expression of NF-κB p65 in the I/R, RIPC and NF-κB activation + RIPC groups were significantly higher than the sham group at T0, T1, T3, T6, T12 and T24 (all $P < 0.05$). **Figure 2** revealed that, in comparison to the I/R and NF-κB activation + RIPC groups, a significant decrease expression of NF-κB p65 protein was observed in the RIPC group at the same time point (T0, T1, T3 and T6) ($P < 0.05$). These results demonstrated that RIPC may inhibit the activation of NF-κB p65.

Positive cell rate in the sham, I/R, RIPC and NF-κB activation + RIPC groups

IHC results demonstrated that positive cell rate in the sham group was 8.78%. At T0, T1, T3, T6, T12 and T24, the positive cell rate in the I/R, RIPC and NF-κB activation + RIPC groups were

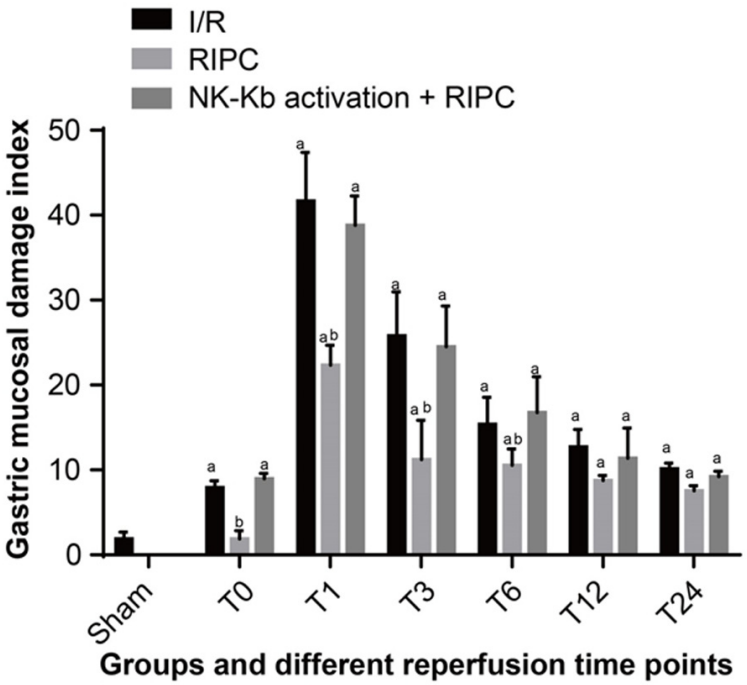

Figure 4. The GMDI among the sham, I/R, RIPC and NF-κB activation + RIPC groups. Notes: GMDI, gastric mucosal damage index; I/R, ischemia/reperfusion; RIPC, remote ischemic preconditioning; NF-κB, nuclear factor kappaB; compared with sham group, [a]$P < 0.05$; compared with I/R group and NF-κB activation + RIPC group at the same time points, [b]$P < 0.05$; compared within groups at T0, [c]$P < 0.05$.

35.53 ± 3.20, 76.91 ± 6.65, 50.37 ± 5.80, 44.21 ± 3.43, 32.94 ± 2.51 and 24.17 ± 2.89; 26.13 ± 2.78, 53.80 ± 6.01, 40.30 ± 4.32, 36.11 ± 2.04, 29.38 ± 2.69 and 20.32 ± 1.17; 32.77 ± 2.91, 69.88 ± 7.05, 47.79 ± 4.80, 45.11 ± 3.77, 30.41 ± 11.19 and 22.44 ± 1.89 respectively. At the same time points (T1, T3, T6, T12 and T24) in comparison to T0, the I/R group, RIPC group and NF-κB activation + RIPC group showed highest positive cell rate at T1 which lowest at T24 (all $P < 0.05$). Compared with sham group, the positive cell rate in the I/R group, RIPC group and NF-κB activation + RIPC group increased markedly at T0, T1, T3, T6, T12 and T24, and had significant differences (all $P < 0.05$). The positive cell rate in RIPC group at T0, T1, T3 and T6 were lower than those in the I/R group and NF-κB activation + RIPC group (all $P < 0.05$) (**Figure 3**).

The GMDI among the sham, I/R, RIPC and NF-κB activation + RIPC groups

The GMDI was 1.89 ± 0.811 points in the sham group. At the six time points of reperfusion (T0, T1, T3, T6, T12 and T24), the GMDI of the I/R group was 7.95 ± 0.78 points, 41.69 ± 5.71 points, 25.83 ± 5.16 points, 15.39 ± 3.17 points, 12.71 ± 2.04 points and 10.14 ± 0.67 points, respectively. At these six time points, the GMDI of the RIPC group was 1.90 ± 0.944 points, 22.37 ± 4.30 points, 11.24 ± 4.61 points, 10.57 ± 3.15 points, 8.78 ± 1.92 points and 7.56 ± 0.59 points, respectively. At these six time points, the GMDIs of the NF-κB + RIPC group was 8.97 ± 0.65 points, 38.80 ± 3.47 points, 24.53 ± 4.78 points, 16.76 ± 4.23 points, 11.39 ± 3.54 points, and 9.21 ± 0.63 points. These results indicated that at the same time points (T0, T1, T3, T6, T12 and T24) there were significantly higher GMDI in the I/R and NF-κB activation + RIPC groups than in the sham group (all $P < 0.05$). No significant difference was observed concerning the GMDI between the I/R and NF-κB activation + RIPC groups ($P > 0.05$). Both these groups had a higher GMDI than the sham group and displayed a decreasing GMDI as time increased. As shown in **Figure 4**, the GMDI of the RIPC group at time points T0, T1, T3 and T6 were significantly lower than those in the I/R and NF-κB activation + RIPC groups (all $P < 0.05$).

Gastric mucosal cell apoptosis rate among the sham, I/R, RIPC and NF-κB activation + RIPC groups

At time point T6 in the sham group there were a few positive apoptotic cells distributed in the epithelium and some layers of the submucosa and glands. In the I/R group, positive apoptotic cells were densely distributed in the mucosa epithelium and glands and its gastric mucosal cell apoptosis rate was significantly higher than that in the sham group ($P < 0.05$). The positive apoptotic cells of the NF-κB activation + RIPC group were mainly distributed in the layers of the mucosa and glands and its apoptosis rate was similar to that of the I/R group ($P < 0.05$). The RIPC group had a remarkably lower apoptosis rate and smaller distribution range of posi-

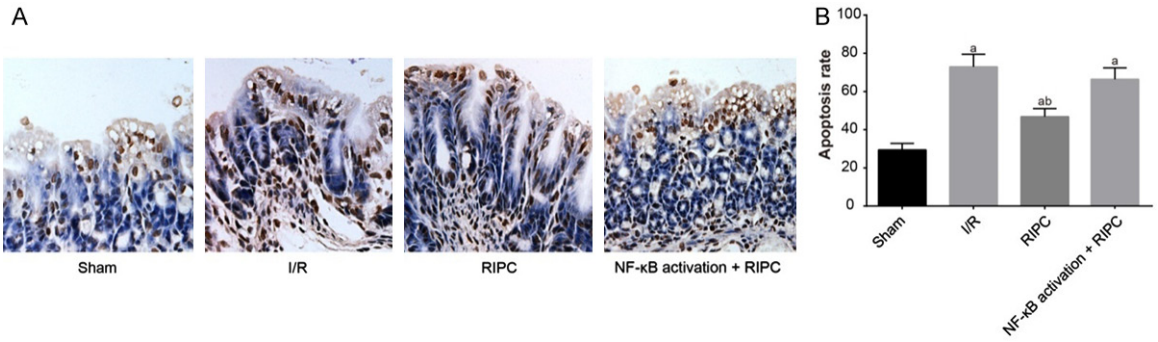

Figure 5. Gastric mucosal cell apoptosis rate (B) among the sham, I/R, RIPC and NF-κB activation + RIPC groupsat T6 under a light microscope (A) (Scale bar = 100 nm). Note: I/R, ischemia/reperfusion; RIPC, remote ischemic preconditioning; NF-κB, nuclear factor kappaB; compared with sham group, $^{a}P < 0.05$; compared with I/R group and NF-κB activation + RIPC group at T0, $^{b}P < 0.05$.

Table 1. Comparisons of MDA level and SOD activity in gastric mucosal tissues of rats among the sham, I/R, RIPC and NF-κB activation + RIPC groups (n = 6, mean ± SD)

Time point	Sham group		I/R group		RIPC group		NF-κB activation + RIPC group	
	MDA (U/mg)	SOD (U/mg)	MDA (U/mg)	SOD (U/mg)	MDA (U/mg)	SOD (U/mg)	MDA (U/mg)	SOD (U/mg)
T0	0.79 ± 0.17	8.38 ± 0.51	3.04 ± 0.15^{a}	6.25 ± 0.54^{a}	2.48 ± 0.15^{a,b}	7.71 ± 0.54^{a,b}	2.88 ± 0.15^{a}	6.25 ± 0.54^{a}
T1	0.76 ± 0.18	8.39 ± 0.47	3.58 ± 0.23^{a,c}	6.30 ± 0.40^{a}	2.43 ± 0.23^{a,b}	7.06 ± 0.31^{a,b,c}	3.68 ± 0.33^{a,c}	6.30 ± 0.40^{a}
T3	0.75 ± 0.18	8.41 ± 0.40	5.49 ± 0.21^{a,c}	6.33 ± 0.49^{a}	2.41 ± 0.32^{a,b}	7.05 ± 0.22^{a,b,c}	6.01 ± 0.22^{a,c}	5.11 ± 0.23^{a,c}
T6	0.78 ± 0.16	8.42 ± 0.42	7.32 ± 0.86^{a,c}	3.61 ± 0.44^{a,c}	4.12 ± 0.27^{a,b,c}	4.26 ± 0.38^{a,b,c}	7.65 ± 0.57^{a,c}	3.88 ± 0.46^{a,c}
T12	0.77 ± 0.12	8.39 ± 0.44	6.86 ± 0.49^{a,c}	3.40 ± 0.46^{a,c}	4.96 ± 0.07^{a,b,c}	5.18 ± 0.42^{a,b,c}	7.02 ± 0.49^{a,c}	3.40 ± 0.46^{a,c}
T24	0.75 ± 0.10	8.43 ± 0.44	6.24 ± 0.15^{a,c}	3.18 ± 0.60^{a,c}	2.99 ± 0.29^{a,b,c}	5.29 ± 0.59^{a,b,c}	6.11 ± 0.18^{a,c}	3.18 ± 0.60^{a,c}

Note: MDA, malondialdehyde; SOD, superoxide dismutase; SD, standard deviation; I/R, ischemia/reperfusion; RIPC, remote ischemic preconditioning; NF-κB, nuclear factor kappaB; T0, 0th h of reperfusion; T1, 1st h of reperfusion; T3, 3rd h of reperfusion; T6, 6th h of reperfusion; T12, 12th h of reperfusion; T24, 24th h of reperfusion; ^{a}, $P < 0.05$ compared with the sham group at the same time point; ^{b}, $P < 0.05$ compared with the I/R group at the same time point; ^{c}, $P < 0.05$ compared with MDA level or SOD activity at T0.

tive apoptotic cells than those in the I/R and NF-κB activation + RIPC groups (both $P < 0.05$) (**Figure 5**).

MDA level and SOD activity in gastric mucosal tissue in the sham, I/R, RIPC and NF-κB activation + RIPC groups

In the I/R group, the MDA level increased with time (T0 < T1 < T3 < T6) and the highest MDA level were observed at T6. The SOD activity increased steadily reaching a peak at T3 and subsequently decreased (T3 > T6 > T12 > T24). In the I/R group, the MDA levels at T1, T3, T6, T12 and T24 and the SOD activities at T6, T12 and T24 were significantly higher than at T0 (all $P < 0.05$). In the RIPC group, the MDA level displayed a decrease-increase-decrease tendency (T0 > T1 > T3, T3 < T6 < T12, T12 > T24). However, the SOD activity had a decrease-increase tendency (T0 > T1 > T3 > T6, T6 < T12 < T24). In the NF-κB activation + RIPC group, the MDA level gradually increased before T6 (T0 < T1 < T3 < T6) and the SOD activity gradually decreased after T1 (T1 > T3 > T6 > T12 > T24). For the same time point (T0, T1, T3, T6, T12 and T24), the I/R, RIPC and NF-κB activation + RIPC groups displayed a higher MDA activity and lower SOD activity than the sham group (all $P < 0.05$). For the same time point (T0, T6, T12 and T24), the RIPC group had a lower MDA level and higher SOD activity than I/R and NF-κB activation + RIPC groups (all $P < 0.05$) (**Table 1**).

Discussion

I-RI refers to the pathological process of cell structure and metabolism impairment caused by an insufficient blood supply to tissues [3, 24]. RIPC is an effective method of treating I-RI and is widely used in the clinical treatment of various organs. However, relevant research on the application of RIPC in GI-RI requires

strengthening. Therefore, this study discusses the effects of RIPC on GI-RI by regulating gastric mucosa NF-κB expression in GI-RI rat models.

The results of this study showed that the RIPC group had less severe gastric mucosal damage, milder edema and congestion of mucosal glands, fewer eosinophils and neutrophils between the muscular layer and glands, as well as a milder congestion in the interstitial blood vessels than the I/R group. In addition, the GMDI and apoptosis rate of gastric mucosal cells in the I/R and NF-κB activation + RIPC groups were significantly higher than those of the sham group. Compared with the IR group, the RIPC group had an evidently lower GMDI and gastric mucosal cell apoptosis rate. Therefore, RIPC can reduce gastric mucosal damage induced by I/R. An imbalance of the active oxygen scavenging system is an important mechanism behind reperfusion injury [25]. Ischemic preconditioning is used as an intervention to attenuate mucosal injury induced by severe I/R [23]. Most importantly, the protective role of RIPC against gastric injury is achieved through the activation of antioxidative mechanisms in the gastric mucosa [16].

This study found that the MDA level was higher and SOD activity was lower in the I/R and RIPC groups than in the sham group. In comparison to the I/R group, the RIPC group exhibited a decreased MDA level and increased SOD activity. This indicates that RIPC can promote SOD activity in the gastric mucosa and reduce MDA levels (especially in the early stage of reperfusion). Ebrahimi et al. demonstrated that reactive oxygen free radicals (OFR) are associated with I-RI and that OFR can lead to I-RI in many organs [26]. I/R-induced gastric mucosal damage is accompanied by the formation of free radicals [27]. The ability of scavenging OFR can be judged from the SOD activity and the MDA level. It also indirectly shows the degree of cell membrane damage being attacked by free oxygen [28]. OFR is considered to be a factor leading of MDA and tissue or cells damage. SOD is a significant member of the antioxidant system and can remove super oxides and prevent I/R-induced gastrointestinal injury [29, 30]. Wang Tao *et al.* found that RIPC can reduce the MDA level and increase SOD activity [31]. This is consistent with the results of our study. We made a hypothesis that RIPC could reduce the MDA level and increase SOD activity in rats with GI-RI, so as to inhibit the production of OFR and protect again I/R induced injuries.

The results also showed that the NF-κB p65 protein levels in the I/R, RIPC and NF-κB activation + RIPC groups were significantly higher than the sham group. However, the RIPC group had a remarkably lower NF-κB p65 protein expression than the I/R and NF-κB activation + RIPC groups. Therefore, RIPC may inhibit NF-κB activation in gastric mucosa tissues. NF-κB is a gene transcription regulatory factor involved in mediating the inflammatory response [19]. In hepatic ischemia and reperfusion, NF-κB is activated and transferred to the nucleus in order to enhance the transcription of a target gene. This may promote the release of TNF-α and IL-1β. NF-κB further enhances the inflammatory response and leads to the increase of white blood cells in the liver and an aggravation of microcirculation disturbance [32]. Blocking the expression of NF-κB can significantly inhibit the production of cerebral I-RI inflammation [33]. Eman *et al.* reported that the inhibition of NF-κB expression through pyrrolidinedithiocarbamate preconditioning contributes to the anti-inflammatory effect and further reduces gastric I/R injury [34]. Therefore, RIPC may inhibit the activation of NF-κB to prevent GI-RI.

In conclusion, this study found that RIPC can attenuate gastric mucosa tissue damage caused by I/R and can be a novel target for GI-RI treatment. In addition, we found that RIPC can reduce the MDA level and increase the SOD activity to inhibit the production of OFR. Furthermore, RIPC may inhibit NF-κB activity via reducing GI-RI. Our study may provide a possible theoretical basis and a novel target for the treatment of ischemia-reperfusion induced gastric injury. However, before clinical application, more evidence and clinical trials are required.

Acknowledgements

We are very grateful for all the advice received on this paper and would like to thank the people involved, without whose support, this study would not have been possible.

Disclosure of conflict of interest

None.

Address correspondence to: Dr. Xing-Yong Wang, Emergency Department, Children's Hospital of Chongqing Medical University, No.136, Second Zhongshan Road, Yuzhong District, Chongqing 400014, P. R. China. Tel: +86-023-63622963; Fax: +86-023-63622963; E-mail: xungyong0517@163.com

References

[1] de Groot H and Rauen U. Ischemia-reperfusion injury: processes in pathogenetic networks: a review. Transplant Proc 2007; 39: 481-484.

[2] Qiao WL, Wang GM, Shi Y, Wu JX, Qi YJ, Zhang JF, Sun H and Yan CD. Differential expression of Bcl-2 and Bax during gastric ischemia-reperfusion of rats. World J Gastroenterol 2011; 17: 1718-1724.

[3] Du DS, Ma XB, Zhang JF, Zhou XY, Li Y, Zhang YM and Qiao WL. The protective effect of capsaicin receptor-mediated genistein postconditioning on gastric ischemia-reperfusion injury in rats. Dig Dis Sci 2010; 55: 3070-3077.

[4] Peskar BM, Ehrlich K, Schuligoi R and Peskar BA. Role of lipoxygenases and lipoxin A(4)/annexin-1 receptor in gastric protection induced by 20% ethanol or sodium salicylate in rats. Pharmacology 2009; 84: 310-313.

[5] Konturek SJ, Brzozowski T, Konturek PC, Schubert ML, Pawlik WW, Padol S and Bayner J. Brain-gut and appetite regulating hormones in the control of gastric secretion and mucosal protection. J Physiol Pharmacol 2008; 59 Suppl 2: 7-31.

[6] Szlachcic A, Brzozowski T, Majka J, Pajdo R, Konturek PC, Pawlik M, Kwiecien S, Drozdowicz D, Bielanski W, Konturek SJ and Pawlik WW. Involvement of orexigenic peptides in the mechanism of gastric mucosal integrity and healing of chronic gastric ulcers. Curr Pharm Des 2010; 16: 1214-1223.

[7] Nakamori Y, Komatsu Y, Kotani T, Kojima S and Takeuchi K. Pathogenic importance of cysteinyl leukotrienes in development of gastric lesions induced by ischemia/reperfusion in mice. J Pharmacol Exp Ther 2010; 333: 91-98.

[8] Suzuki S, Suzuki H, Horiguchi K, Tsugawa H, Matsuzaki J, Takagi T, Shimojima N and Hibi T. Delayed gastric emptying and disruption of the interstitial cells of Cajal network after gastric ischaemia and reperfusion. Neurogastroenterol Motil 2010; 22: 585-593, e126.

[9] Hausenloy DJ and Yellon DM. Remote ischaemic preconditioning: underlying mechanisms and clinical application. Cardiovasc Res 2008; 79: 377-386.

[10] Walsh SR, Tang T, Sadat U, Dutka DP and Gaunt ME. Cardioprotection by remote ischaemic preconditioning. Br J Anaesth 2007; 99: 611-616.

[11] Ali ZA, Callaghan CJ, Lim E, Ali AA, Nouraei SA, Akthar AM, Boyle JR, Varty K, Kharbanda RK, Dutka DP and Gaunt ME. Remote ischemic preconditioning reduces myocardial and renal injury after elective abdominal aortic aneurysm repair: a randomized controlled trial. Circulation 2007; 116: I98-105.

[12] Choi YS, Shim JK, Kim JC, Kang KS, Seo YH, Ahn KR and Kwak YL. Effect of remote ischemic preconditioning on renal dysfunction after complex valvular heart surgery: a randomized controlled trial. J Thorac Cardiovasc Surg 2011; 142: 148-154.

[13] Rahman IA, Mascaro JG, Steeds RP, Frenneaux MP, Nightingale P, Gosling P, Townsend P, Townend JN, Green D and Bonser RS. Remote ischemic preconditioning in human coronary artery bypass surgery: from promise to disappointment? Circulation 2010; 122: S53-59.

[14] Pickard JM, Botker HE, Crimi G, Davidson B, Davidson SM, Dutka D, Ferdinandy P, Ganske R, Garcia-Dorado D, Giricz Z, Gourine AV, Heusch G, Kharbanda R, Kleinbongard P, MacAllister R, McIntyre C, Meybohm P, Prunier F, Redington A, Robertson NJ, Suleiman MS, Vanezis A, Walsh S, Yellon DM and Hausenloy DJ. Remote ischemic conditioning: from experimental observation to clinical application: report from the 8th biennial hatter cardiovascular institute workshop. Basic Res Cardiol 2015; 110: 453.

[15] Wang F, Birch SE, He R, Tawadros P, Szaszi K, Kapus A and Rotstein OD. Remote ischemic preconditioning by hindlimb occlusion prevents liver ischemic/reperfusion injury: the role of high mobility group-box 1. Ann Surg 2010; 251: 292-299.

[16] Bobryshev P, Bagaeva T and Filaretova L. Ischemic preconditioning attenuates gastric ischemia-reperfusion injury through involvement of glucocorticoids. J Physiol Pharmacol 2009; 60 Suppl 7: 155-160.

[17] He G and Karin M. NF-kappaB and STAT3-key players in liver inflammation and cancer. Cell Res 2011; 21: 159-168.

[18] Oeckinghaus A and Ghosh S. The NF-kappaB family of transcription factors and its regulation. Cold Spring Harb Perspect Biol 2009; 1: a000034.

[19] Lawrence T. The nuclear factor NF-kappaB pathway in inflammation. Cold Spring Harb Perspect Biol 2009; 1: a001651.

[20] Mustonen H, Hietaranta A, Puolakkainen P, Kemppainen E, Paimela H, Kiviluoto T and Kivilaakso E. Ethanol induced NF-{kappa}B activation protects against cell injury in cultured rat gastric mucosal epithelium. Am J Physiol Gas-

trointest Liver Physiol 2007; 292: G1614-1621.
[21] Shin HJ, Won NH and Lee HW. Remote ischemic preconditioning prevents lipopolysaccharide-induced liver injury through inhibition of NF-kappaB activation in mice. J Anesth 2014; 28: 898-905.
[22] Zhang JF, Zhang YM, Yan CD and Zhou XP. Neuroregulative mechanism of hypothalamic paraventricular nucleus on gastric ischemia-reperfusion injury in rats. Life Sci 2002; 71: 1501-1510.
[23] Brzozowski T, Konturek PC, Konturek SJ, Pajdo R, Kwiecien S, Pawlik M, Drozdowicz D, Sliwowski Z and Pawlik WW. Ischemic preconditioning of remote organs attenuates gastric ischemia-reperfusion injury through involvement of prostaglandins and sensory nerves. Eur J Pharmacol 2004; 499: 201-213.
[24] Zhai Y, Busuttil RW and Kupiec-Weglinski JW. Liver ischemia and reperfusion injury: new insights into mechanisms of innate-adaptive immune-mediated tissue inflammation. Am J Transplant 2011; 11: 1563-1569.
[25] Tsutsumi YM, Yokoyama T, Horikawa Y, Roth DM and Patel HH. Reactive oxygen species trigger ischemic and pharmacological postconditioning: in vivo and in vitro characterization. Life Sci 2007; 81: 1223-1227.
[26] Ebrahimi A, Salimi F, Safaei M, Melali H, Jazi AH, Nematbakhsh M, Mokhtari N and Rasooli H. How effective are alprostadil and hydrocortisone on reperfusion injury in kidney after distant organ ischemia? J Res Med Sci 2013; 18: 755-758.
[27] Pan JS, He SZ, Xu HZ, Zhan XJ, Yang XN, Xiao HM, Shi HX and Ren JL. Oxidative stress disturbs energy metabolism of mitochondria in ethanol-induced gastric mucosa injury. World J Gastroenterol 2008; 14: 5857-5867.
[28] Wang H F ZXH, Shi W. Study of malondialdehyde (MDA) content, superoxide dismutase (SOD) and glutathione peroxidase (GSH-Px) activities in chickens infected with avian infectious bronchitis virus. African Journal of Biotechnology 2011; 10: 9213-9217.
[29] Drabko K, Bojarska-Junak A and Kowalczyk J. [Activity of superoxide dismutase and glutathione peroxidase and concentrations of malonyldialdehyde, vitamin E, total antioxidant status and extracellular cytokines concentrations in children with acute lymphoblastic leukaemia (ALL)]. Med Wieku Rozwoj 2006; 10: 861-868.
[30] Suzuki H, Nishizawa T, Tsugawa H, Mogami S and Hibi T. Roles of oxidative stress in stomach disorders. J Clin Biochem Nutr 2012; 50: 35-39.
[31] Wang T, Zhou YT, Chen XN, Zhu AX and Wu BH. Remote ischemic postconditioning protects against gastric mucosal lesions in rats. World J Gastroenterol 2014; 20: 9519-9527.
[32] Shin T, Kuboki S and Lentsch AB. Roles of nuclear factor-kappaB in postischemic liver. Hepatol Res 2008; 38: 429-440.
[33] Zhang P, Liu X, Zhu Y, Chen S, Zhou D and Wang Y. Honokiol inhibits the inflammatory reaction during cerebral ischemia reperfusion by suppressing NF-kappaB activation and cytokine production of glial cells. Neurosci Lett 2013; 534: 123-127.
[34] El Eter E, Hagar HH, Al-Tuwaijiri A and Arafa M. Nuclear factor-kappaB inhibition by pyrrolidinedithiocarbamate attenuates gastric ischemia-reperfusion injury in rats. Can J Physiol Pharmacol 2005; 83: 483-492.